

Suppression of Auger recombination in long-wavelength quantum well W-structure lasers

P. C. Findlay, J-P. R. Wells,* I. V. Bradley,* J. G. Crowder, and C. R. Pidgeon†
Physics Department, Heriot Watt University, Edinburgh EH14 4AS, United Kingdom

B. N. Murdin
Physics Department, University of Surrey, Guildford GU2 5XH, United Kingdom

M. J. Yang, I. Vurgaftman, and J. R. Meyer
Naval Research Laboratory, Washington DC 20375
 (Received 14 February 2000)

Using picosecond pulses from a free-electron laser, we have carried out a pump-probe determination of Shockley-Read-Hall (SRH) and Auger free-carrier recombination lifetimes in two long-wave (6–7 μm) W-structure laser with $\text{InAs}/\text{Ga}_{1-x}\text{In}_x\text{Sb}/\text{InAs}/\text{AlSb}$ active regions. The SRH coefficient is nearly constant ($A \approx 4.0 \times 10^8 \text{ s}^{-1}$), while the Auger coefficient has an upper limit of $C = 4.0 \times 10^{-27}$ to $2.2 \times 10^{-27} \text{ cm}^6/\text{s}$ in the temperature range 40–230 K. This represents an order of magnitude Auger suppression compared to type-I III-V semiconductors with the same energy gap.

I. INTRODUCTION

As is well known, the ability to control the Auger recombination rate in narrow-gap semiconductor systems, either by direct device design^{1–3} (involving carrier extraction and exclusion) or by band structure engineering,^{4–8} is critical to a number of important applications for which the Auger process fundamentally limits the performance. Low-threshold nonlinear devices controlled by cw lasers and high-sensitivity mid-infrared detectors and emitters need long excess carrier lifetimes, whereas applications such as laser mode locking, ultrafast radiation detectors, and optical switches require recovery times as short as possible. Despite the fact that intersubband quantum well detectors and quantum cascade (QC) lasers have been operated very successfully at long wavelengths (superlattice QC lasers out to 17 μm have been reported⁹), interband narrow-gap detectors and lasers are generally the most attractive option in the 5 μm region. For example, pulsed $\text{InSb}/\text{In}_{1-x}\text{Al}_x\text{Sb}$ heterostructure diodes at 5.1 μm ³ and optically pumped type-II quantum well lasers⁶ have operated well above 77 K, and recently so-called type-II W structures have lased in cw mode in the 6 μm region at 210 K.¹⁰

Type-(II) quantum well (QW) lasers employing $\text{InAs}/\text{GaInSb}$ active regions have been known for a number of years to show great promise for the mid-infrared (MIR) spectral region,¹¹ in part because the so-called CHHS Auger transitions [i.e., where the conduction-to-heavy-hole (CH) recombination is accompanied by a heavy-to-split-off-hole transition] are eliminated by effectively removing the resonance between the energy gap E_g and spin-orbit splitting Δ_0 . In particular, the type-II W multiple quantum well (named for the shape of the four-constituent conduction band profile of the $\text{InAs}/\text{Ga}_{1-x}\text{In}_x\text{Sb}/\text{InAs}/\text{AlSb}$ active region) preserves the large optical matrix elements of the $\text{InAs}/\text{Ga}_{1-x}\text{In}_x\text{Sb}$ superlattice while yielding the preferred two-dimensional (2D) dispersion relations for both electrons and holes.¹² Optically pumped W-shaped lasers have recently operated in cw

mode out to wavelengths as long as 7.1 μm , and are predicted by computer simulations to be attractive for operation at still longer wavelengths beyond 25 μm .¹³

We earlier reported the utilization of rf linac-pumped free-electron lasers (FEL's) to study Auger recombination, and particularly its deliberate suppression, in arsenic-rich $\text{InAs}/\text{InAs}_{1-x}\text{Sb}_x$ type-II strained-layer superlattices at room temperature,¹⁴ by comparison with similar measurements^{15,16} on epilayers of bulk $\text{Hg}_{1-x}\text{Cd}_x\text{Te}$ with the same cutoff wavelength near 10 μm . Lifetimes for type-II W lasers were derived previously by correlating the experimental threshold intensities for optically pumped lasing with calculated threshold carrier concentrations.^{17,18} However, those experiments did not yield an independent determination of the Shockley-Read-Hall (SRH) and Auger contributions, since at each temperature T the lifetime could be obtained for only one special carrier density corresponding to the lasing threshold at that T . In the present study, we have used the more direct pump-probe measurement technique to independently determine the SRH contribution and an upper limit on the Auger contribution for the temperature range from 40 to 230 K.

II. EXPERIMENT

Two W-structure laser samples were grown by molecular-beam epitaxy on p -GaSb substrates at NRL, using procedures described elsewhere.¹⁹ The active regions contained 70 four-constituent periods consisting of $\text{InAs}(25 \text{ \AA})/\text{Ga}_{0.7}\text{In}_{0.3}\text{Sb}(24 \text{ \AA})/\text{InAs}(25 \text{ \AA})/\text{AlSb}(42 \text{ \AA})$ for sample N5 and $\text{InAs}(28 \text{ \AA})/\text{Ga}_{0.64}\text{In}_{0.36}\text{Sb}(22 \text{ \AA})/\text{InAs}(28 \text{ \AA})/\text{AlSb}(42 \text{ \AA})$ for sample N8, which were surrounded by AlSb bottom and top optical cladding layers and GaSb buffer and cap layers. Lasing properties of the two structures were reported previously.¹⁸ The present wavelength-degenerate pump-probe transmission experiments were performed with the Dutch FEL in Utrecht (FELIX), which operates with pulse trains ("macropulses") of typical length 4 μs and at a repetition rate of 5 Hz. The macropulse consists of a train of "micropulses," each of adjustable width in the range 2–10

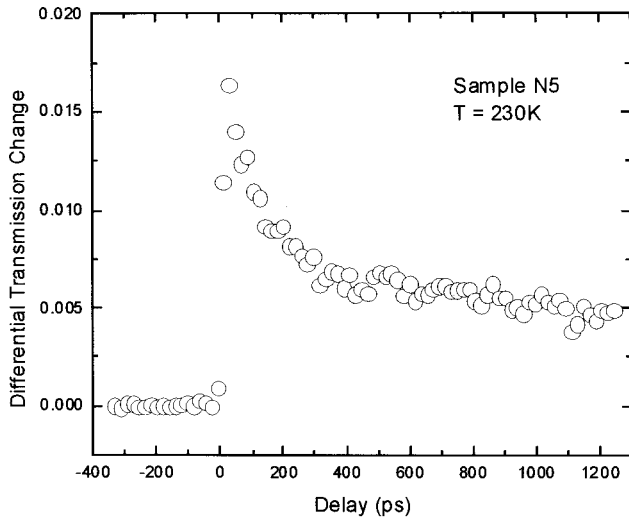


FIG. 1. Three-beam measurement of probe differential transmission change versus delay time for sample N5 at $T=230$ K, pump wavelength $4.5 \mu\text{m}$.

ps and separated by 40 ns. It was shown previously^{14,16} that, for the excitation conditions used throughout this study, carrier temperatures approach the lattice temperature to within 2% in less than 3 ps, which results in a temperature increase in the sample of only ~ 0.02 K per pulse. Hence, we have neglected heating effects and, for recombination processes occurring in less than about 20 ns (see below), have interpreted the data in terms of independent single pulses.

The macropulse fluctuations of FELIX, which depend strongly on the required performance of the machine, are typically of the order of a few percent. In order to obtain a good signal-to-noise ratio in the MIR regime, we utilized a pump-probe method that compensates for these macropulse fluctuations. The experimental arrangement consisted of a three-beam pump-probe-reference setup that has been described in detail elsewhere.¹⁶ The result was a signal/noise ratio better than 0.1%, even when the fluctuations from macropulse to macropulse were several percent. The three beams were focused on the sample using an $f=25$ cm parabolic mirror, which resulted in a spot size of $100 \mu\text{m}$. The effective pump and probe energy fluences per micropulse were estimated to be 350 and $10 \mu\text{J}/\text{cm}^2$, respectively, including losses due to beam splitters and optics. The relative transmittance of the probe was measured directly as a function of optical delay t between the pump and probe pulses. The sample was mounted in a flow cryostat (4–300 K).

As the pump radiation is absorbed, band filling causes a strong dynamic blueshift in the IR absorption edge (the dynamic Moss-Burstein shift) and leads to pronounced bleaching near the excitation frequency.^{16,20} Recovery times in the range 20–1200 ps were found and shown to be strongly dependent on both the sample temperature and the excited carrier density. Typical pump-probe transmission data for W laser sample N5 are shown in Fig. 1, taken at 230 K with a pump wavelength of $4.5 \mu\text{m}$. We find that at all temperatures stimulated radiative emission represents the most efficient recombination mechanism for probe delays of up to 100 ps, while nonradiative processes dominate at times longer than 100 ps. The pump-probe technique then allows a direct measurement of the excited carrier density as a function of time

as the excited carriers recombine. By contrast with our earlier work on bulk materials,¹⁶ we find that even at room temperature both the SRH and Auger processes make a significant contribution to the nonradiative recombination at low excitation levels. Analysis of the recovery of the probe absorption leads to a determination of the recombination coefficients as described below.

III. ANALYSIS

In order to interpret the raw data of probe transmission versus probe delay time we need to convert the measured transmission into values of excited carrier concentration $N_e(t)$.^{14–16} The rate of decay of $N_e(t)$ with pump-probe delay can then be extracted directly, and the SRH and Auger recombination coefficients obtained by fitting $N_e(t)$ with a simple rate equation. The pump pulse drives apart the electron and hole quasi-Fermi energies and bleaches the transmission. While the bleaching is not necessarily complete, a shorter pump wavelength maximizes the possible separation of the quasi-Fermi energies. For any given wavelength, each transmission value corresponds to a unique photoexcited electron and hole concentration, $N_e = N_h$. The analysis uses a knowledge of the band structure¹⁸ and small-signal absorption cross section to calculate the density of states and hence the transmission as a function of carrier concentration. Since the measured lifetimes are substantially longer than the pulse duration (5 ps), the generation rate is zero during the probe pulse delay time. The recombination rate, which is some function of $N_e(t)$, can then be measured unambiguously.

The pulse duration may similarly be neglected [i.e., the probe pulse shape function $I(t)$ is effectively a δ function] when we calculate the sample transmission

$$T(\hbar\omega, t) \propto \exp[-\alpha(\hbar\omega, t)d], \quad (1)$$

where $\hbar\omega$ is the photon energy and d is the active thickness. We assume that the absorption coefficient α , while time and wavelength dependent, is spatially constant through the probed region of the sample. This is a good approximation because the initial concentration would be spatially uniform for complete bleaching. Note that, while the probe reflectivity is complicated by the varying refractive indices of the cladding, active, and substrate layers of the laser structure, this does not significantly influence the results of our signal processing, which takes the ratio of the measured difference in the probe and reference transmission to the reference transmission. The reflectivities cancel (apart from a small optically induced contribution), and we are left with an expression that relies solely on the change in the absorption coefficient, $\Delta\alpha$, induced by the pump.

The data analysis procedure incorporates our knowledge of the band structure for the W-structure quantum wells,¹⁸ which governs the (final and initial) electron and hole energies (E_e and E_h) for the optical transitions at a given photon energy, and also the density of states functions (g_e and g_h , both of which may include contributions from multiple subbands). The band structure is calculated using an eight-band $\mathbf{k}\cdot\mathbf{p}$ calculation resulting in the required in-plane two-dimensional dispersion relation. Inspection of the calculated band structure determines that the energy range available in the present experiment results in only transitions involving

the electron and heavy-hole subbands. The 2D density of states function we take to be $g_e = m_e/2\pi\hbar^2$.

For a range of electron Fermi energies, one then computes the corresponding hole Fermi energies and electron and hole excited carrier concentrations from the relation

$$N_e = \int_{E_c}^{\infty} f_e(E)g_e(E)dE = \int_{-\infty}^{E_v^h} f_h(E)g_h(E)dE, \quad (2)$$

where f_e and f_h are the Fermi occupation probability functions for electrons and holes, respectively, and E_c and E_v are the conduction and valence band edge energies. This gives two-dimensional excited carrier concentrations which, if we are to compare with bulk materials, require a conversion to three dimensions. To find the corresponding three-dimensional excited carrier concentrations N_{3D} , we use the expression $N_{3D} = N_{2D}/L$, where N_{2D} is the sheet density per four-constituent period of the W structure and L is the period thickness.¹⁰ At the same time, each assumed value of electron Fermi energy determines a unique value of α (and hence T) from the relation

$$\alpha = \sigma[1 - f_e(E_e) - f_h(E_h)]J_{cv}(\hbar\omega), \quad (3)$$

where $\hbar\omega = E_e - E_h$, $J_{cv}(\hbar\omega)$ is the joint density of states, and the absorption cross section σ is normally determined by fitting the theoretical transmission corresponding to the equilibrium Fermi energy to the small-signal absorption spectrum taken with a Fourier-transform spectrometer. However, this has not been possible for the present W-structure lasers because the active layer is too thin to make a good absolute determination of α from the transmission measurements. We therefore derived σ from a theoretical analysis of the lasing characteristics.¹⁸ We again use the relation $\sigma_{3D} = \sigma_{2D}/L$.

We can now calculate the value of the excited carrier concentration $N_e(t)$ corresponding to each value of transmission $T(t)$. As described previously, we have also included the effect of small refractive index changes arising from a shift in the plasma frequency.¹⁵ Figure 2 shows a typical plot of N_e versus t_{delay} corresponding to the raw transmission data in Fig. 1 (sample N6). For the region below the threshold concentration for stimulated emission, the dynamics may be approximated by the simple rate equation

$$\frac{1}{N_e} \frac{dN_e(t)}{dt} = A + BN_e(t) + CN_e^2(t), \quad (4)$$

where A , B , and C are the SRH, radiative, and Auger recombination coefficients, respectively, for a nondegenerate N_e distribution. For these laser samples amplified spontaneous emission (ASE) occurs at quite low values of N_e , when

$$E_f^c + E_f^v > 0. \quad (5)$$

In an inverted sample, spontaneously emitted photons are amplified by the presence of ASE. This results in an exponential increase in the number of photons and a decrease of the excited carrier density, which produces the sharp rise in the recombination rate observed in Fig. 2 at carrier densities above $3.7 \times 10^{17} \text{ cm}^{-3}$. We note that the value of $N_e(t)$ at which we see the onset of rapid decay almost exactly coincides with the concentration determined for lasing threshold in these samples ($N_e = 5 \times 10^{17} \text{ cm}^{-3}$).^{17,18} We can do a

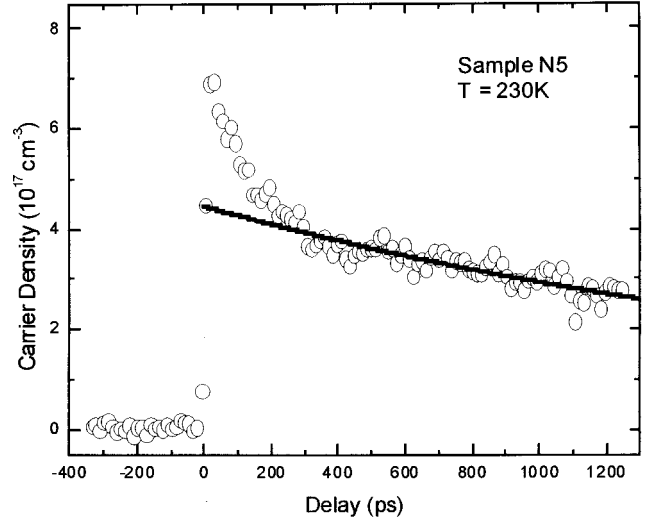


FIG. 2. Computed excited carrier concentration N_e versus t_{delay} obtained from the pump-probe transmission results of Fig. 1, as described in the text. The solid curve is a simple exponential fit to the equation $dN_e/dt = AN_e$.

back-of-the-envelope calculation to justify this interpretation as follows. The increase in recombination rate per carrier due to ASE is

$$\frac{1}{N_s} \frac{dN_s}{dt} = \frac{\beta P}{N_s}, \quad (6)$$

where N_s is the spontaneous carrier density, β is the gain, and P is the photon density. The last is given by²¹

$$P = \frac{P_0}{\beta} [\exp(\beta L) - 1], \quad (7)$$

where P_0 is the spontaneously emitted photon density captured by the waveguide and L is the length of the pumped section. Based on the excited carrier density we estimate that βL ranges up to at least 5. The total spontaneously emitted photon density per unit time (i.e., N_s/τ_s , where τ_s is the spontaneous emission time—a few nanoseconds at these concentrations¹²) is $\sim 10^{25} \text{ cm}^{-3} \text{ s}^{-1}$. Assuming that a reasonable fraction of this actually stays in the waveguide, we get an upper bound of about 10^{10} s^{-1} for the increase in recombination rate per carrier due to ASE. The actual increase we observe is $\sim 5 \times 10^9 \text{ s}^{-1}$, which we believe is reasonable to attribute to ASE.

From previous work¹⁴⁻¹⁶ we estimate the radiative recombination to be negligible in this concentration range. Unfortunately, given the limited range of data in Fig. 2 available for fitting, we cannot distinguish between a simple exponential fit and the full fit of Eq. (4). Thus, we make a simple exponential fit $dN_e/dt = AN_e$ to the data to obtain the SRH coefficient $A = 4 \times 10^8 \text{ s}^{-1}$. We then obtain an upper limit for C as follows. The full equation to be fitted to the low-concentration portion of the curve is $dN_e/dt = AN_e + CN_e^3$. This equation can be integrated analytically to obtain

$$N_e = [k \exp(2At) - C/A]^{-1/2}, \quad (8)$$

where k is a constant of the integration. Taking Eq. (8) and successively reducing the value of A (to unphysically small values in order to obtain an upper bound on C), it is found that C tends toward an asymptotic value of $4.0 \times 10^{-27} \text{ cm}^6 \text{ s}^{-1}$. This implies that the actual value of C is significantly suppressed compared to type-I III-V semiconductors with the same cutoff wavelength of $6.1 \mu\text{m}$ for sample N5 and $7.3 \mu\text{m}$ for sample N8.^{17,18} It has been pointed out that suppression via the valence band engineering is not expected to be strong in these samples,¹⁷ particularly at room temperature where thermal and inhomogeneity broadening are important. However, there is clearly significant Auger suppression, much of which arises from suppression of the so-called CCCH process [i.e., where the CH recombination is accompanied by an electron transition to higher-energy conduction-band state (CC)], resulting from the type-II band alignment—i.e., the resultant “narrow” gap is created from two comparatively large-gap component layers.

IV. CONCLUSION

Summarizing, we have utilized a picosecond free-electron laser to measure directly the SRH recombination rates for

two long-wavelength W-structure laser samples with InAs/Ga_{1-x}In_xSb/InAs/AlSb active regions in the temperature range 40–230 K. We have determined an upper bound on the Auger coefficient to be $4.0 \times 10^{-27} \text{ cm}^6 \text{ s}^{-1}$ in the temperature range 40–230 K. This represents a suppression of the Auger coefficient by about an order of magnitude compared to type-I semiconductor systems with the same energy gap.¹⁷ The SRH coefficient is $A = 4.0 \times 10^8 \text{ s}^{-1}$. These results provide clear confirmation that Auger recombination is strongly suppressed in long-wavelength ($\lambda > 5 \mu\text{m}$) type-II-quantum wells. This consequence of band structure engineering will become even more important when laser operation is attempted at wavelengths as long as $25 \mu\text{m}$.¹³

ACKNOWLEDGMENTS

We acknowledge EPSRC for support of this work (J.P. W., I.V.B., and P.C.F.). We are grateful to DERA Malvern for financial support (P.C.F.). The authors gratefully acknowledge the support of the Stichting voor Fundamenteel Onderzoek der Materie (FOM) in providing the required beam time on FELIX, and highly appreciate the skilful assistance of the FELIX staff, in particular Dr. A. F. G. van der Meer. NRL acknowledges ONR for support of this work.

*Also at FOM-Institute for Plasma Physics “Rijnhuizen,” P.O. Box 1207, 3430 BE Nieuwegein, The Netherlands.

†Corresponding author: FAX: 0131 451 3136; Email address: c.r.pidgeon@hw.ac.uk

¹A. M. White, *Infrared Phys.* **25**, 729 (1985).

²T. Ashley, A. B. Dean, C. T. Elliott, A. D. Johnson, G. J. Pryce, A. M. White, and C. R. Whitehouse, *Semicond. Sci. Technol.* **8**, 386 (1993); *Appl. Phys. Lett.* **64**, 2433 (1994).

³T. Ashley, C. T. Elliott, R. Jeffries, A. D. Johnson, G. G. Pryce, A. M. White, and M. Carroll, *Appl. Phys. Lett.* **70**, 931 (1997).

⁴E. R. Youngdale, J. R. Meyer, C. A. Hoffman, F. J. Bartoli, C. H. Grein, P. M. Young, H. Ehrenreich, R. H. Miles, and D. H. Chow, *Appl. Phys. Lett.* **64**, 3160 (1994).

⁵R. M. Biefeld, A. A. Allerman, S. R. Kurtz, and J. H. Burkhart, *J. Electron. Mater.* **26**, 1225 (1997).

⁶M. E. Flatté, T. C. Hassenberg, J. T. Olesberg, S. A. Anson, T. F. Boggess, C. Yan, and D. L. McDaniel, Jr., *Appl. Phys. Lett.* **71**, 3764 (1997).

⁷C. R. Pidgeon, B. N. Murdin, and C. Ciesla, *Prog. Quantum Electron.* **21**, 361 (1998).

⁸J. R. Meyer, L. J. Olafsen, E. H. Aifer, W. W. Bewley, C. L. Felix, I. Vurgaftman, M. J. Yang, L. Goldberg, D. Zhang, D.-H. Lin, S. S. Pei, and D. H. Chow, *IEEE Proc.: Optoelectron.* **145**, 275 (1998).

⁹A. Tredicucci, C. Gmachl, F. Capasso, D. L. Sivco, A. L. Hutchinson, and A. Y. Cho, *Appl. Phys. Lett.* **74**, 638 (1999).

¹⁰C. L. Felix, W. W. Bewley, L. J. Olafsen, D. W. Stokes, W. H. Aifer, I. Vurgaftman, J. R. Meyer, and M. J. Yang, *IEEE Photonics Technol. Lett.* **8**, 964 (1999).

¹¹C. H. Grein, P. M. Young, and H. Ehrenreich, *J. Appl. Phys.* **76**,

1940 (1994).

¹²J. R. Meyer, C. A. Hoffman, F. J. Bartoli, and L. R. Ram-Mohan, *Appl. Phys. Lett.* **67**, 757 (1995).

¹³I. Vurgaftman and J. R. Meyer, *Appl. Phys. Lett.* **75**, 899 (1999).

¹⁴C. M. Ciesla, B. N. Murdin, C. R. Pidgeon, R. A. Stradling, C. C. Phillips, M. Livingstone, I. Galbraith, D. A. Jaroszynski, C. J. G. M. Langerak, P. J. P. Tang, and M. J. Pullin, *J. Appl. Phys.* **80**, 2994 (1996).

¹⁵C. M. Ciesla, B. N. Murdin, T. J. Phillips, A. M. White, A. R. Beattie, C. J. G. M. Langerak, C. T. Elliott, C. R. Pidgeon, and S. Sivananthan, *Appl. Phys. Lett.* **71**, 491 (1997).

¹⁶P. C. Findlay, C. R. Pidgeon, R. Kotitschke, A. Hollingworth, B. N. Murdin, C. M. Langerak, A. F. G. van der Meer, C. M. Ciesla, J. Oswald, A. Homer, G. Springholz, and G. Bauer, *Phys. Rev. B* **58**, 12 908 (1998).

¹⁷J. R. Meyer, C. L. Felix, W. W. Bewley, I. Vurgaftman, E. H. Aifer, L. J. Olafsen, J. R. Lindle, C. A. Hoffman, M.-J. Yang, B. R. Bennett, B. V. Shanabrook, H. Lee, C.-H. Lin, S. S. Pei, and R. H. Miles, *Appl. Phys. Lett.* **73**, 2857 (1998).

¹⁸D. W. Stokes, L. J. Olafsen, W. W. Bewley, I. Vurgaftman, C. L. Felix, E. H. Aifer, J. R. Meyer, and M. J. Yang, *J. Appl. Phys.* **86**, 4729 (1999).

¹⁹M. J. Yang, W. J. Moore, B. R. Bennett, B. V. Shanabrook, J. O. Cross, W. W. Bewley, C. L. Felix, I. Vurgaftman, and J. R. Meyer, *J. Appl. Phys.* **86**, 1796 (1999).

²⁰M. E. Flatté, C. H. Grein, T. C. Hassenberg, S. A. Anson, D.-J. Jang, J. T. Olesberg, and T. F. Boggess, *Phys. Rev. B* **59**, 5745 (1999).

²¹T. P. Lee, C. A. Burrus, and B. I. Miller, *IEEE J. Quantum Electron.* **QE9**, 820 (1973).